Cyclic *trans*-stilbenes: synthesis, structural and spectroscopic characterization, photophysical and photochemical properties †

Michael Oelgemöller,[a] Bernhard Brem,[b] Rudolf Frank,[c] Siegfried Schneider,*[b] Dieter Lenoir,*[c] Norbert Hertkorn,[c] Yumi Origane,[a] Peter Lemmen,[d] Johann Lex[e] and Yoshihisa Inoue*[a]

[a] *Inoue Photochirogenesis Project, ERATO, JST, 4-6-3 Kamishinden, Toyonaka-shi, 560-0085 Osaka, Japan. E-mail: inoue@chem.eng.osaka-u.ac.jp; Fax: +81 6 6836 1636; Tel: +81 6 6836 0063*

[b] *Institut für Physikalische und Theoretische Chemie, Friedrich-Alexander-Universität, Egerlandstr. 3, D-91058 Erlangen, Germany. E-mail: schneider@chemie.uni-erlangen.de; Fax: +49 9131 852 8307; Tel: +49 9131 852 7341*

[c] *Institut für Ökologische Chemie, GSF-Forschungszentrum Neuherberg, D-85758 Oberschleißheim, Germany. E-mail: lenoir@gsf.de; Fax: +49 89 318 73371; Tel: +49 89 318 72960*

[d] *Institut für Organische Chemie und Biochemie, Technische Universität München, Lichtenbergstr. 4, D-85747 Garching, Germany. E-mail: Peter.Lemmen@ch.tum.de; Fax: +49 89 289 13329; Tel: +49 89 289 13319*

[e] *Institut für Organische Chemie, Universität zu Köln, Greinstr. 4, D-50939 Köln, Germany. E-mail: Johann.Lex@uni-koeln.de; Fax: +49 221 470 5057; Tel: +49 221 470 3091*

Received (in Cambridge, UK) 2nd April 2002, Accepted 12th July 2002
First published as an Advance Article on the web 14th August 2002

trans-Stilbene and several cyclic derivatives with hindered free rotation around the C(vinyl)–C(phenyl) single bond were studied by various spectroscopic techniques. Those derivatives which contain 6- or 7-membered aliphatic rings do not exhibit any measurable $S_1 \longrightarrow S_0$ fluorescence. The introduction of two methoxy groups into the 6-membered aliphatic ring derivative accelerates its photoreactivity to such an extent that fluorescence or resonance Raman spectroscopy investigations become impossible. The introduction of aliphatic rings has only a little effect on the frequency of the phenyl-ring stretching vibrations, but pronounced ones on the IR and Raman intensities. The frequency of the vinylic stretching mode is downshifted between 5 and 100 cm^{-1} except in the case of the derivative with the 4-membered ring, which experiences a hypsochromic shift of 80 cm^{-1}. Only *trans*-stilbene and its 4-membered cyclic analogues were amenable to fluorescence lifetime measurements. Analysis of VT-NMR spectra of stilbene **7** reveals a barrier of 15.9 kcal mol^{-1} for equilibration of aliphatic equatorial and axial H-atoms.

Introduction

During the last decades, the photoinduced *trans–cis* isomerization of *trans*-stilbene and its derivatives has become the most intensively studied photochemical reaction and a major test for theoretical models of activated barrier crossing.[1] In a number of reports,[2] cyclic stilbene derivatives have been investigated as model substrates since the torsion around the single bond is hindered in these systems.‡ Additionally, cyclic stilbenes were recently used as *light driven molecular rotors*,[3] and have been successfully applied for enantiodifferentiating photoisomerizations in the presence of chiral sensitizers.[4] Due to the limited availability of these substrates, a detailed comparative study on cyclic stilbenes is still missing so far. This contribution aims to fill this gap, and the synthesis and characterization of several cyclic stilbene derivatives as well as the results from steady-state and time-resolved spectroscopic investigations are presented.

Results and discussion

Synthesis of starting materials

Besides *trans*-stilbene **1** and its di-*tert*-butyl derivative **12**, ten cyclic compounds were chosen for this study (Chart 1). The syntheses of four derivatives have been described earlier: the truly *stiff* stilbenes **2**[5] and **3**[6b] in which two 5- or 6-membered rings block the rotation around both the single and double bond, and the derivatives **5** and **6** in which these rings block rotations solely around the single bond.§ *trans*-1-(1-Indanylidene)indane **5**,[6c] *trans*-1-(1-tetralinylidene)tetralin¶ **6**,[7] *trans*-2,2,2′,2′-tetramethyl-1-(1-tetralinylidene)tetralin **9**[7] and *trans*-di-*tert*-butylstilbene **12**[8] were prepared according to literature procedures. All other stilbene derivatives were synthesized by reductive coupling of the corresponding ketones with low valent titanium (McMurry coupling).[9] For the synthesis of derivative **8**, two different ketones, *i.e.* 1-indanone and 1-tetralone in a 2 : 1 ratio, were coupled. In most cases, mixtures of both isomers were obtained, which needed to be separated by chromatography or (in the case of **4**) by HPLC, respectively.

The corresponding diol, a common side-product in the McMurry reaction, was obtained in larger amounts only during the synthesis of stilbene **4**. Inspection of the crude reaction mixture by ^{1}H-NMR spectroscopy showed a 6 : 4 ratio of desired **4** (as a *ca.* 1 : 1 mixture of both isomers) and diol **13**. From the preparation of **5**, compound **14** was isolated as a minor product in about 5% yield (Chart 2) as unambiguously

† Dedicated to the memory of Professor Sang-Chul Shim.
‡ All these previous studies mainly focused on compounds **2** and **5** (Chart 1), respectively.
§ In previous publications,[2] compound **5** was termed a *stiff* stilbene although it can isomerize.
¶ Tetralin is 1,2,3,4-tetrahydronaphthalene.

 DOI: 10.1039/b203167a

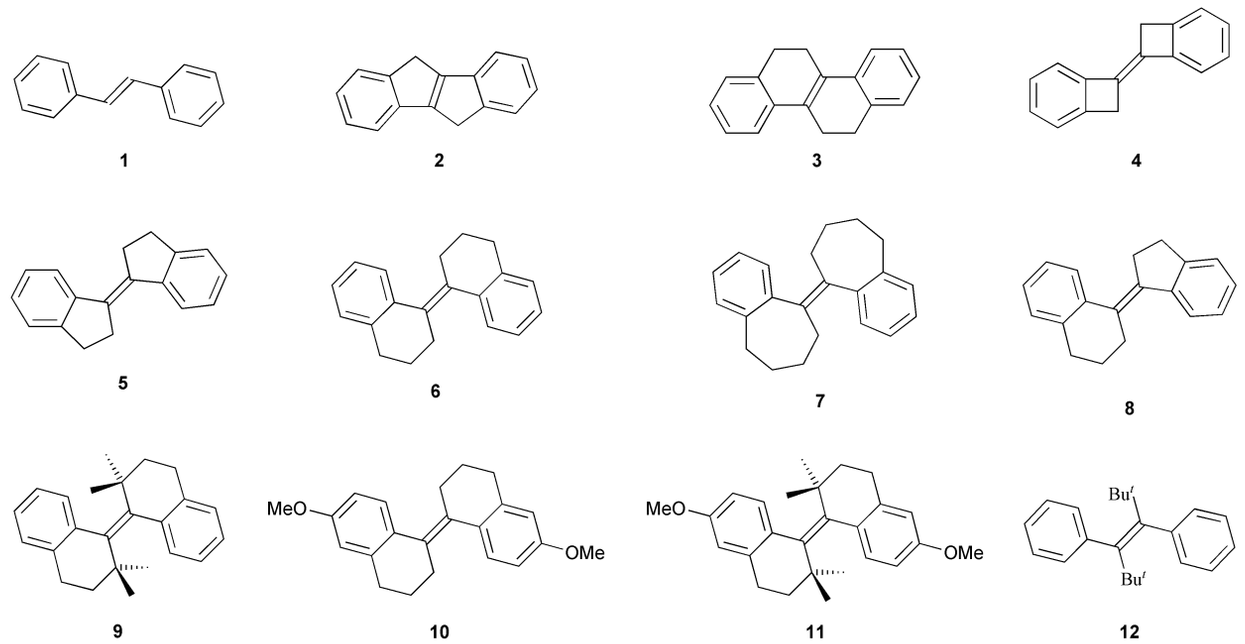

Chart 1 Selected *trans*-stilbene derivatives.

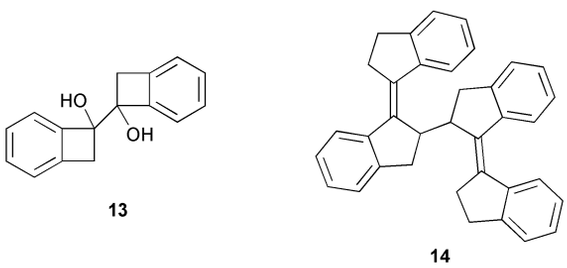

Chart 2 Important by-products.

proven by X-ray structure analysis.[10a] The structure of **14** is remarkable since it contains both isomeric forms (*cis* and *trans*) of the **5** units inside the same molecule.

Calculated ground state geometries and crystal structures

Three important structural parameters are commonly used for the description of stilbene derivatives (Scheme 1): the torsion

Scheme 1

angles around the double (Θ) and the single bond (ϕ), and the C=C bond distance (r), respectively.[11] The results from the calculations and X-ray structure analyses are summarized in Table 1.

As expected from structural considerations, the model calculations (PM3 hamiltonian) predict that besides the *stiff* stilbenes **2** and **3** solely the derivatives incorporating the 4- and 5-membered rings are planar (**4**) or fairly planar (**5**) both with respect to torsion around the double (Θ) and the single bond (ϕ). For **4** (Fig. 1) and **5**,[17b] the planarity was proven by X-ray structure analysis.‖ The derivatives carrying 6- and 7-membered aliphatic rings (**6** and **7**) exhibit a pronounced torsion around the single bond (calc. $\phi = 40°$ and 71°), whereas the double bond twist is, however, significant only in compound **6** (calc. $\Theta = 9°$). While the stilbenes **2** and **3** show only one stable conformation, derivatives **5**–**7** possess several geometric conformations due to the increasing flexibility of the aliphatic rings with increasing ring size.[12] In **6**, a geometrical heterogeneity must be additionally taken into account since each 6-membered ring can adopt two nearly isoenergetic conformations, thus giving rise to two groups of molecules possessing either C_1 or C_2 symmetry. This structural heterogeneity is less pronounced in the smaller cyclic derivatives. As shown by Ogawa and co-workers, the conformational flexibility of **6** is also expressed in its solid state structure.[13] Although both aliphatic 6-membered rings in **6** adopt a twist-boat-like conformation, they nevertheless show significant differences in these geometries. Most interestingly one of the aliphatic rings shows an extreme disorder which was explained on the basis of packing differences in the crystal.

The conformational flexibility in solution is largest for the 7-membered ring-containing stilbene **7** as can be seen by its broad and unresolved signals in the ^{1}H-NMR. On the other hand, restricted rotation of the 7-membered rings in *trans*-stilbene **7** is revealed from a complex temperature dependence of its ^{1}H- and ^{13}C-NMR spectra. The aliphatic part of the 400 MHz ^{1}H-NMR spectrum in DMSO-d_6 at intermediate temperatures (T < 373 K) shows several exchange processes and is characterized by multiple episodes of coalescence and line broadening. At T > 393 K the geminal protons are equilibrated, but couplings are not fully resolved even at T = 423 K in DMSO-d_6. The room temperature (303 K) 500 MHz ^{1}H-NMR spectrum of **7** in D_3CNO_2 showed an array of resolved broad aliphatic resonances, closely resembling those of the 400 MHz ^{1}H-NMR spectrum of **7** in DMSO-d_6 at 303 K, which could be assigned from the cross peak positions in the

‖ *Crystal data*: $C_{16}H_{12}$ (from *n*-hexane–methanol, mp 181–183 °C) **4**: M = 204.26, monoclinic, space group $P2_1/c$, a = 12.259(1), b = 5.283(1), c = 8.856(1) Å, β = 101.07(1)°, V = 562.88(13) Å^3; Z = 2; Mo Kα radiation, 2297 reflections measured, 968 reflections with $I > 2\sigma(I)$, R_1 = 0.041, wR_2 = 0.111. CCDC reference number 182508. See http://www.rsc.org/suppdata/p2/b2/b203167a/ for crystallographic files in .cif format.

Crystal data: $C_{22}H_{24}$ (from *n*-hexane, mp 179–180 °C) **7**: M = 288.41, monoclinic, space group $P2_1/n$, a = 10.726(1), b = 7.282(1), c = 10.756(1) Å, β = 106.29(1)°, V = 806.39(15) Å^3; Z = 2; Mo Kα radiation, 3305 reflections measured, 1481 reflections with $I > 2\sigma(I)$, R_1 = 0.036, wR_2 = 0.094. CCDC reference number 182507. See http://www.rsc.org/suppdata/p2/b2/b203167a/ for crystallographic files in .cif format.

Crystal data: $C_{22}H_{24}O_2$ (from *n*-hexane, mp 210–211 °C) **10**: M = 320.41, monoclinic, space group $C2/c$, a = 26.192(1), b = 9.483(1), c = 6.913(1) Å, β = 101.3(1)°, V = 1683.9(3) Å^3; Z = **4**; Mo Kα radiation, 3490 reflections measured, 1469 reflections with $I > 2\sigma(I)$, R_1 = 0.041, wR_2 = 0.110. CCDC reference number 182509. See http://www.rsc.org/suppdata/p2/b2/b203167a/ for crystallographic files in .cif format.

Table 1 Calculated (PM3 hamiltonian) and measured ground and excited state properties of **1**–**12**. Average torsion angles Θ and ϕ, bond length r (ground state), and wavelength λ_m of the $S_0 \longrightarrow S_1$ absorption band. Included are the experimental values of the absorption maxima (in *n*-hexane) and the 0–0-transition in emission

Compound	Point group	Θ/° calc./exp.	ϕ/° calc./exp.	r/Å calc./exp.	λ_m/nm exp./calc. (fluorescence)
1	C_{2h}	0/0 [a]	0/5 [a]	1.342/1.318 [a]	322 [e]/326 (334 [e])
2	C_{2h}	0	0	1.374	330 [e]/352 (345 [e])
3	C_i	0/0 [a]	16/17 [a]	1.354/1.353(4) [a]	339 [e]/344 (354 [e])
4	C_{2b}	0/0 [b]	0/0 [b]	1.319/1.326(6) [b]	323 [e]/309 (329 [e])
5	C_i	0/0, 0 [a,d]	9/1, 0 [a,d]	1.345/1.334(3), 1.349(3) [a,d]	339 [e]/333 (344 [e])
6	C_2 [c]	9/6 [a]	40/46 [a]	1.351/1.347(3) [a]	286/318
7	C_2	0/0 [b]	71/70 [b]	1.346/1.347(4) [b]	272/280
8	C_1	3	12, 36	1.349	313/326
9	C_2	37/37 [a]	33/45 [a]	1.361/1.364 [a]	310/355
10	C_1	9/17 [b]	39/37 [b]	1.352/1.361(34) [b]	296/333
11	C_1	37	33	1.364	314/368
12	C_1	1/0,0 [a,d]	91/92, 91 [a,d]	1.353/1.329(11), 1.346(5) [a,d]	267/228

[a] Values taken from X-ray structure analysis: **1**,[17a] **3**,[10b] **5**,[17b] **6**,[13] **9**[16b] and **12**.[16a] [b] From X-ray structure analysis of **4**, **7** and **10**. [c] Several conformations with similar ΔH_f (see text). [d] Two independent molecules. [e] Values refer to 0–0-transition.

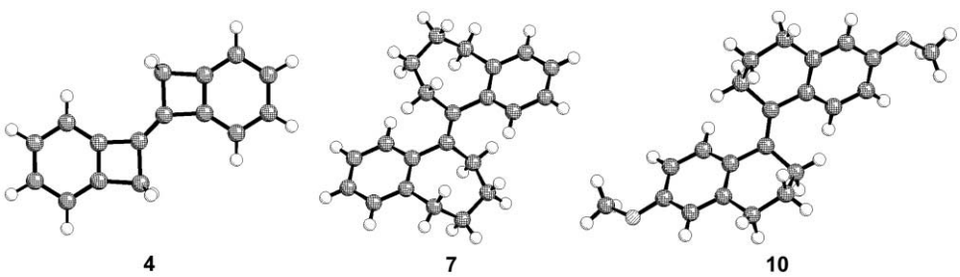

Fig. 1 Molecular structures of **4**, **7** and **10** as determined by X-ray diffraction (Schakal-97 plots).

HSQC NMR spectrum. This assignment was corroborated by COSY and NOESY spectra; the latter showed strong exchange cross peaks of geminal protons at t_m = 50 and 450 ms at 303 K, respectively. The average proton chemical shift of equatorial and axial protons H-2 (2.91 ppm), H-5 (2.24 ppm), H-3 (1.65 ppm) and H-4 (1.49 ppm) in D_3CNO_2 at room temperature is very close to that of the high temperature limit (443 K) in DMSO-d_6, which then could be assigned according to Fig. 2. Fine structure of proton NMR resonances at 423 K in DMSO-d_6 is best resolved for allylic H-2 and H-4 and almost not recognizable for H-5, respectively.

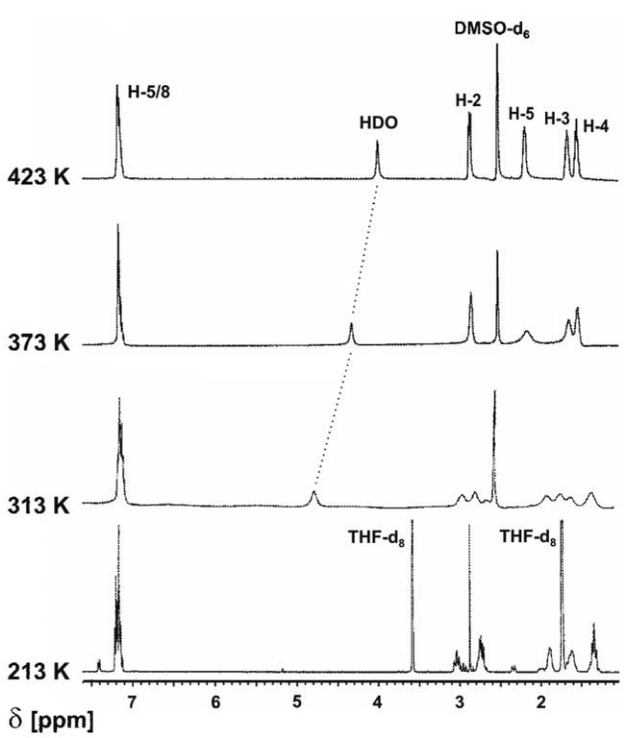

Fig. 2 VT-^{1}H-NMR spectra of **7** in DMSO-d_6 and THF-d_8 at temperatures given.

On lowering the temperature, H-5 broadens most strongly and coalesces at 343 K, followed by H-3 and less pronouncedly by H-4 and H-2, which reaches coalescence at T_c = 325 K. The free energy of activation for the process to render these diastereotopic equatorial and axial protons at C-2 equivalent is $\Delta G^{\ddagger}_{325}$ = 15.9 kcal mol^{-1} and the process that interconverts these protons can be reasonably assigned to be ring inversion (atropisomerism about sp^3–sp^3 single bonds within the seven membered ring). At no temperature between 423 K (DMSO-d_6) and 183 K (D_3CNO_2) could coupling constants be resolved in the 400 MHz proton NMR spectra for the protons H-3 and H-4 of compound **7**, respectively. The four aromatic protons are merged into a complex resonance (δ = 7.1–7.25 ppm) in the temperature range 303–433 K (DMSO-d_6). In THF-d_8 solution an additional minor (15% of main conformer) low field (δ = 7.43 ppm) resonance occurs, which splits into a doublet at T < 275 K and most probably represents H-9.

The 100 MHz ^{13}C-NMR spectrum in DMSO-d_6 was best resolved at T near 363 K and showed four aliphatic methylene, four aromatic methine and three quaternary (aromatic and vinyl) carbon atoms, which could be readily assigned according to their chemical shift values. When proceeding to higher temperature (reversible) broadening occurred, degrading resolution for all protonated carbon atoms at 443 K almost beyond recognition. When lowering the temperature, broadening occurred for all resonances in the ^{13}C-NMR spectrum with C-4 being most affected: while being broadened already at 363 K, it became unrecognizable at T = 323 K and below. At 303 K in DMSO-d_6, no ^{13}C-NMR resonances could be observed in the entire spectrum of compound **7**.

Seven membered rings feature complex pseudorotational equilibria with rather low barriers which in the case of **7** become enlarged by fused aromatic rings and an allylic exocyclic double bond capable of electronic interaction. While separate twist-boat and chair conformers of benzocycloheptene have not been observed by ^{1}H-NMR,[14] various types of ring

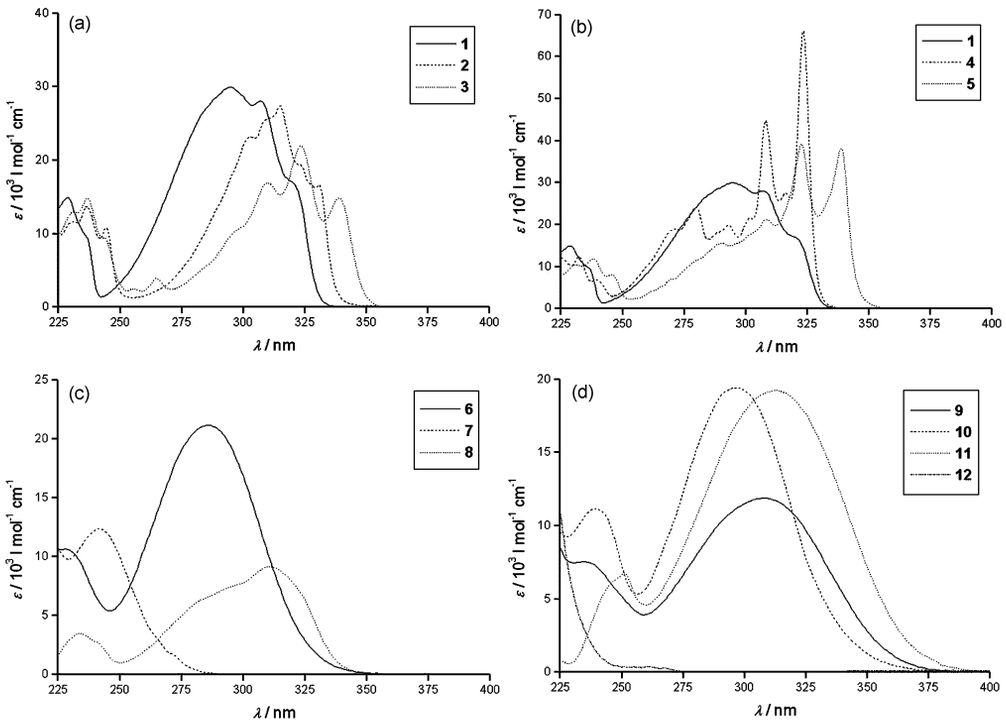

Fig. 3 UV/Vis absorption spectra of **1**–**12** in *n*-hexane.

heteroatom substitution provide enough rigidity to allow observation of conformational isomers such as chair, twist-chair, boat and twist-boat, respectively, by ^{1}H- and ^{13}C-NMR techniques at low temperature.[15] According to AM1 calculations ΔH_f of the chair (C), boat (B) and twist-boat (TB) conformations of **7** increases by 4.3 kcal mol^{-1} (from C to B) and by another 5.2 kcal mol^{-1} (from B to TB), respectively. Van der Waals interactions of protons H-2 and H-9 probably cause an increase of the torsion angle for the central double bond from 1.2° (C), 0.5° (B) to 11.7° (TB). To the best of our knowledge compound **7** is the first example of a pure hydrocarbon in which a seven membered ring shows dynamic NMR behavior, but the absence of resolved coupling constants, clean slow conformational equilibria (the feasible low temperature limit was 190 K) and the dominance of chemical exchange in NOESY spectra precluded an exhaustive description of individual conformational rearrangements.

Methoxy substitution at the aromatic ring as in **10** has no effect on the bond twist (although a marginal effect was found in the crystal structure: Θ = 17°), but introduction of two methyl groups at each C-2 and C-2′ as in **9** and **11** has. The double bond twisting angle in **9** and **11** is calculated as about Θ = 37°, the calculated length of the vinylic bond is significantly increased (1.364 Å as in **11** *vs.* 1.319 Å as in **4**). Single crystal structure analysis performed for compound **9** nicely confirmed the calculated large deviations from planarity (crystal structure: Θ = 37°, ϕ = 45°).[16b] For **12**, the solid state structure (two independent molecules) showed that the incorporation of two *tert*-butyl groups at the central double bond causes the phenyl groups to rotate in such a way that the planes of the C=C bond and of the phenyl rings become perpendicular.[16a] This was also found for the solid state structure of the *cis*-isomer of **12**, in which the π-systems of the phenyl groups are additionally cofacial.[16d]

Steady-state absorption and emission spectra

The observed bathochromic shift in the UV/Vis absorption spectra of the *stiff* stilbenes **2** and **3** of approximately 10 and 20 nm with respect to the parent *trans*-stilbene (Fig. 3a) is predicted correctly by the quantum chemical calculations for **3**, but not for **2**. As one would expect in view of the similarity in calculated ground state geometry, compounds **4** and **5** exhibit UV/Vis absorption spectra which are also similar to that of *trans*-stilbene itself, except that the vibrational structure is well pronounced already at room temperature (Fig. 3b).** The statement about the vibrational structure is, at least to some extent, also true for derivatives **2** and **3** and can be taken as evidence that the torsion around the single bond (ϕ) causes the reduction in vibrational structure in the absorption spectrum of *trans*-stilbene.[18] Whereas **5** shows a pronounced bathochromic shift of the 0–0-transition of about 17 nm relative to **1** (predicted value 7 nm), about the same excitation energy is found in **4** (in contrast to the predicted hypsochromic shift of about 15 nm). The longest wavelength absorption band of **6** (Fig. 3c) peaks around 286 nm (predicted 318 nm), but does not show any vibrational structure at all, not even in low temperature solution. A reasonable explanation for the disappearance of the vibronic structure can be structural heterogeneity, since each 6-membered ring can adopt two different geometries (*vide supra*). This yields 4 different isomers with comparable total energy and slightly different excitation energies. The absorption spectrum of **7** (Fig. 3c) has a certain similarity with that of benzene, showing a strong absorption band around 242 nm and a weak one around 272 nm. This observation can be understood in view of the decreased coupling between the π-electronic systems of the two phenyl rings and that of the double bond. The absorption spectrum of **12** (Fig. 3d) shows essentially the features of the benzene spectrum. The longest wavelength transition (L_a type) shows up as a very weak band ($\nu \approx 37500$ cm^{-1} or λ = 267 nm) next to a strong band with a maximum around 41000 cm^{-1} (235 nm). This bathochromic shift compared to the benzene $B_{a,b}$ transition should originate from electrostatic coupling with the π-electrons of the vinyl group. The presence of one 6-membered aliphatic ring is already sufficient to suppress the appearance of vibrational structure in the UV/Vis absorption spectra as demonstrated in Fig. 3c for compound **8**. Thus, it is also not surprising that none

** It should be mentioned here that **4** used for the present investigations contained both *trans* and *cis* isomer. The different experiments are sensitive to a different extent to the *cis* impurity, but most important for us, fluorescence of the *cis* isomer is extremely weak.

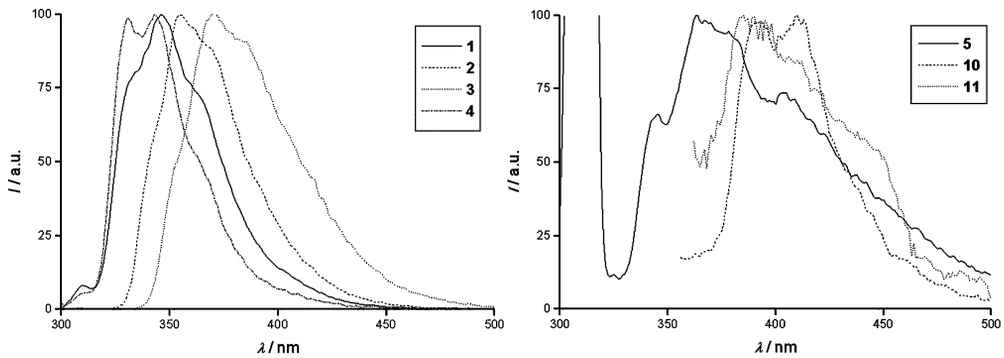

Fig. 4 Fluorescence spectra of **1**–**5** in *n*-hexane (excitation wavelength 308 nm) and photoproducts of **10** and **11** (photolysis at 308 nm).

of the derivatives **9**–**11** (Fig. 3d) shows vibrational structure in the absorption spectra.

The incorporation of the two methyl groups into the aliphatic bridge has a significant effect on the absorption maximum. It causes a 24 nm bathochromic shift if **9** is compared to **6** and a 20 nm shift in the dimethoxy derivatives (**11** *vs.* **10**). A bathochromic shift is well established also for methoxy-substitution in the *para* position.[1] It appears smaller for the pair **9/11** (5 nm) than for **6/10** (10 nm). In comparison, methoxy-substitution in the *para* position of compound **4** yields a bathochromic shift of the 0–0-transition of about 20 nm.[32a]

The fluorescence spectra of the *stiff* stilbenes **2** and **3** (Fig. 4a) show a bathochromic shift corresponding to that observed in the absorption spectra. Since isomerization around the double bond is prevented, the fluorescence quantum yield approaches unity (for **3**, see ref. 1). The great similarity in geometry (and absorption spectra) between **1** and **4** is also reflected in the stationary fluorescence spectra (Fig. 4a). The fluorescence yield of **4** is, however, somewhat higher than that of *trans*-stilbene **1** (0.06 *vs.* 0.036 in *n*-hexane and 0.05 *vs.* 0.016 in polar solvents[19]). In accordance with the observed 17 nm bathochromic shift of the 0–0-absorption band of **5** *vs.* **1**, a bathochromic shift also appears in the fluorescence spectrum, but is less pronounced, namely about 10 nm (Fig. 4b). This can be taken as evidence that the extent of geometrical relaxation in the excited state is different for the various derivatives leading at least to different Franck–Condon factors for the radiative $S_1 \longrightarrow S_0$ transition (the emission spectrum of **5** extends much more to the red). The stationary fluorescence yields of **5** are significantly lower (0.025 in *n*-hexane; 0.02 in methanol and acetonitrile) than those of *trans*-stilbene itself, indicating that the 5-membered ring even accelerates isomerization.[20] Hohlneicher and co-workers recently reported fluorescence spectra of **4** and **5** matrix-isolated at 15 K in argon, and the low frequency modes were analyzed in comparison with Raman spectra.[21] These authors stated that "the most striking difference with respect to the parent stilbene is the lack of pronounced progressions of low frequency a_g modes in the fused ring derivatives".

No stationary fluorescence emission could be observed from derivatives **6**–**11**, which contain at least one 6- or 7-membered bridging ring. In the case of compound **7**, this lack of fluorescence can be rationalized by the assumption that the longest wavelength transition has a very low transition dipole moment and concomitantly a very low rate for radiative decay. In compounds **6** and **9**–**11**, the longest wavelength transition appears as a broad and intense band, for which an analogous line of argument cannot necessarily be used (calculations predict the longest wavelength transitions to have an oscillatory strength *f* in the range of 0.5–1.0[32a]).

In accordance with the observation described above, the derivatives **10** and **11** exhibit no fluorescence. In an attempt to record fluorescence decay curves by means of the single photon timing technique,[20] prolonged irradiation of **10** or **11** in *n*-hexane under an argon atmosphere caused, however, photochemical reactions, and the final photoproduct(s) showed emission in the 360–500 nm range (Fig. 4b). The lack of vibronic structure in the emission spectra of the photoproduct(s) can either be related to the still existing presence of the methoxy groups, or to the existence of more than one product. The lifetime data (*vide infra*) indeed provide evidence that in both cases at least two different products were formed. An attempt was made to identify the photolysis products by GC/MS coupling techniques. The crude product mixture obtained from the photolysis of **10** contained *ca.* 80% unreactive starting material besides numerous photoproducts formed mainly due to degradation. The *cis*-isomer could not be detected, which can be explained by its thermal re-isomerization or further cyclization and oxidation to the corresponding phenanthrene **15** (Scheme 2). In general, this

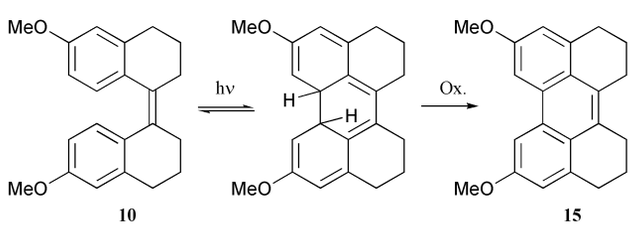

Scheme 2

photocyclization/oxidation cascade is widely observed in the photochemistry of stilbenes, and proceeds easily already in the presence of traces of oxidant.[22]

The formation of the phenanthrene is supported by the GC/MS analysis as the more polar main product shows a peak with m/z = 318 corresponding to the M^+-peak of compound **15**. To further verify this assumption, **10** was irradiated in *n*-hexane at 300 ± 10 nm under non-degassed conditions, and the progress of the reaction was followed by UV/Vis spectroscopy (Fig. 5).

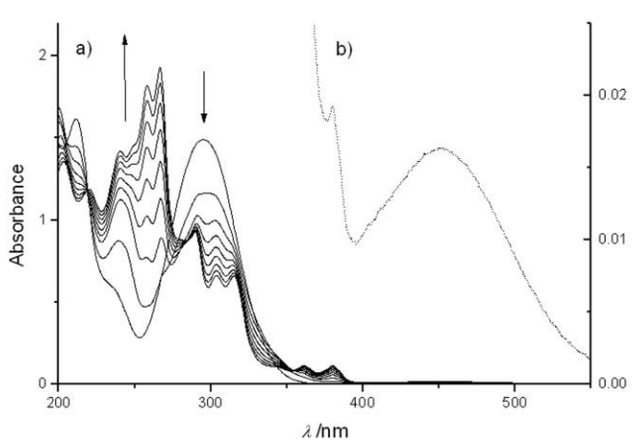

Fig. 5 UV/Vis-spectral changes upon photolysis of **10**; a) after stepwise irradiation for 0–8 min; b) immediately after 1 min of irradiation (enlarged).

When the spectrum was recorded immediately after 1 min of irradiation, the characteristic absorption of the dihydrophenanthrene of **10** could be observed at 450 nm (Fig. 5b). This absorption disappeared totally after *ca.* 10 min standing at room-temperature in the dark, and instead, the strong bands of the phenanthrene appeared at 258 and 267 nm, respectively, unambiguously proving further oxidation.

Although photocyclization can be assumed for compounds **4**–**8** and **10**, it was found to be a major reaction pathway solely for **6** and **10**, respectively.[23] This indicates that the *cis*-isomers of these two compounds have optimal distances between the inner C-8 and C-8′ positions for photocyclization, and further oxidation easily occurs even after careful degassing with an inert gas prior to irradiation.

Upon photolysis of **11** only unselective photodecomposition was observed. The intermediary formed *cis*-isomer of the structurally related stilbene **9** readily re-isomerizes to the more stable *trans*-form, †† and only starting material can be recovered after irradiation.[16] Thus, efficient *trans–cis*-isomerization can be also ruled out for compound **11**. As a conclusion compounds **9** and **11** possess sterically protected double bonds, which cannot undergo any further cyclization reactions.

IR and Raman spectroscopy

The division of the investigated compounds into three groups is also useful for the discussion of their vibronic spectra. Although discussion will focus mainly on the bands in the double bond stretching region, the Raman and IR spectra are shown in the full range between 900 and 1800 cm^{-1} (Fig. 6).

In the IR spectrum of *trans*-stilbene **1**, the bands of medium intensity at 1597 and 1578 cm^{-1} are assigned to the *anti*-symmetrical linear combination of benzene modes 8a and 8b (according to the Varsanyi nomenclature[24]), whereas in the Raman spectrum, the bands at 1638, 1598 and the shoulder around 1578 cm^{-1} represent the vinylic stretch and the symmetrical linear combination of these modes.[25] The normal mode calculations with the down-scaled force field reproduce the experimental frequencies of *trans*-stilbene **1** fairly well (Table 2; Fig. 7). In compound **12**, the benzene rings are only weakly coupled. Therefore, the bands originating from phenyl vibrations appear in the range between 1575 and 1601 cm^{-1} as in mono-substituted benzene and *trans*-stilbene. In the lower frequency region there are pronounced differences in the IR spectra, mainly because of the contribution of the *tert*-butyl groups, whose vibrations are not enhanced in the Raman spectra, and the lack of the vibrations of the vinylic hydrogens. Interesting to note is the disappearance of the strong IR-stilbene mode around 965 cm^{-1}. To our great surprise, the vinylic C=C stretching mode of **12** is not observed in the Raman spectrum recorded with λ_{ex} = 380 nm. One possible explanation might be that the wavefunction of the lowest excited state comprises only the two phenyl rings. Enhancement of the Raman cross section due to (*pre*-)resonance with this state would then exclude the vinylic stretch, since the bond order would not be changed upon electronic excitation in such a state (A-term scattering according to Albrecht's theory [26]). The normal mode calculations predict the vinylic C=C double bond stretch around 1655 cm^{-1}. Thus, the benzene ring vibrations around 1600 cm^{-1} and below should not cover it.

In the *stiff* stilbenes, π-conjugation should be maximized. Because of the concomitant decrease in π-bond order of the ethylenic double bond, a significant decrease in the vinylic stretching frequency and eventually small shifts in the phenyl ring vibrations due to the changed substitution pattern can be expected. The two linear combinations of the 8a phenyl ring modes can be easily identified by their near degeneracy in the IR and Raman spectra (ν = 1604 cm^{-1} in **2**, and 1600 cm^{-1} in **3**). The vinyl stretching mode should appear only in the Raman spectrum. The most reasonable candidates are therefore the 1554 cm^{-1} (compound **2**) and 1617 cm^{-1} (compound **3**) bands. From the normal coordinate calculations it is assumed that compound **2** adopts C_{2h} symmetry. In compound **3**, in which the rotation around the single and double bond is hindered by two 6-membered aliphatic rings, the symmetry of the system can be C_1, C_2 or C_i depending on the conformation of the two bridges. The calculated normal mode frequencies are not very sensitive to the actual geometry, whereas IR intensities slightly depend on it. The given assignment is in acceptable agreement with the theoretical results, although the vinyl stretch in **3** is calculated to be as high as in **1**. The very high intensity of the 1563 and the 1490 cm^{-1} Raman bands of **3** is additionally surprising.

Since the vibrational structure in the UV/Vis absorption spectra of **4** and **5** is different with respect to intensity distribution, the observation of large differences in their IR and Raman spectra is not surprising. The Raman spectrum of **5** resembles that of *trans*-stilbene **1** with the vinyl-stretch at 1633 cm^{-1} and the phenyl-stretch at 1594 cm^{-1}. In the 4-ring system **4**, both bands appear strongly shifted with the phenyl-stretch at 1584 cm^{-1} and the vinyl-stretch at 1718 cm^{-1}, respectively. The frequency shift of the latter mode (80 cm^{-1}) is about half of that predicted by the normal mode calculations (182 cm^{-1} *vs.* stilbene). The phenyl mode of **4** appears at lower frequency (1584 *vs.* 1598 cm^{-1}), but is calculated to be at significantly higher frequency (1635 *vs.* 1590 cm^{-1}). In contrast to the experimental observations, the calculated frequency shifts for **5** are also significant (vinylic stretch: $\Delta\nu$ = 59 cm^{-1}, phenylic stretch $\Delta\nu$ = 20 cm^{-1}). In the IR spectra of **4**, no bands are observed in the double bond region, whereas only one is found in the case of **5**. The location of the latter is in excellent agreement with that found in stilbene (1597 cm^{-1}). One must, therefore, conclude that the phenyl ring modes are not drastically shifted in frequency. But due to the aliphatic bridge, the local symmetry is perturbed and consequently, the intensities changed (the intensity pattern of phenyl modes is known to be characteristic for the substitution pattern[24]). The frequencies assigned to the ethylenic stretch in **4** and **5** are much higher than the spacing in the progressions observed in the low temperature fluorescence spectra of these compounds, *i.e.* 1655 cm^{-1} (for **4**) and 1575 cm^{-1} (for **5**).[27] Although it has been suggested that these progressions are caused by the vinyl stretching vibration, we believe in our assignment, since further evidence is provided by comparison with the spectra of the methoxy derivative of compound **4**. This derivative exhibits also two strong Raman bands at 1600 and 1734 cm^{-1}, thus showing a substituent effect on the vinylic stretching frequency.[32]

The apparent reduction in IR intensity of the phenyl modes is also observed for the derivatives **6** and **7**. The normal mode originating from the benzene 8a vibration is fairly weak, its position nearly constant. The mode derived from 8b can only be assumed by comparison due to its extreme weakness, and seems to shift somewhat. In the Raman spectra, it appears that the phenyl mode based on the 8a benzene vibration conserves its location in both species, but the intensity does so only in the case of compound **6**. The vinyl mode frequency of compound **7** is essentially equal to that of *trans*-stilbene **1**, whereas in derivative **6**, no (strong) Raman band is found which could be reasonably assigned to this mode (except if one assumes a superposition with the phenylic mode around 1600 cm^{-1}). In this connection, it is important to note that the Raman and IR spectra of **6** and **9** exhibit pronounced differences. Because of the appearance of one band each, in the IR and Raman spectra around 1565 and 1595 cm^{-1}, respectively, it should be reasonable to assign these to the benzene 8a and 8b based normal modes. The strong band around 1540 cm^{-1} has no counterpart in the IR spectrum and should therefore be assigned to the

†† For **9**, the *cis*-isomer was observed *via* low-temperature NMR during irradiation.[16d]

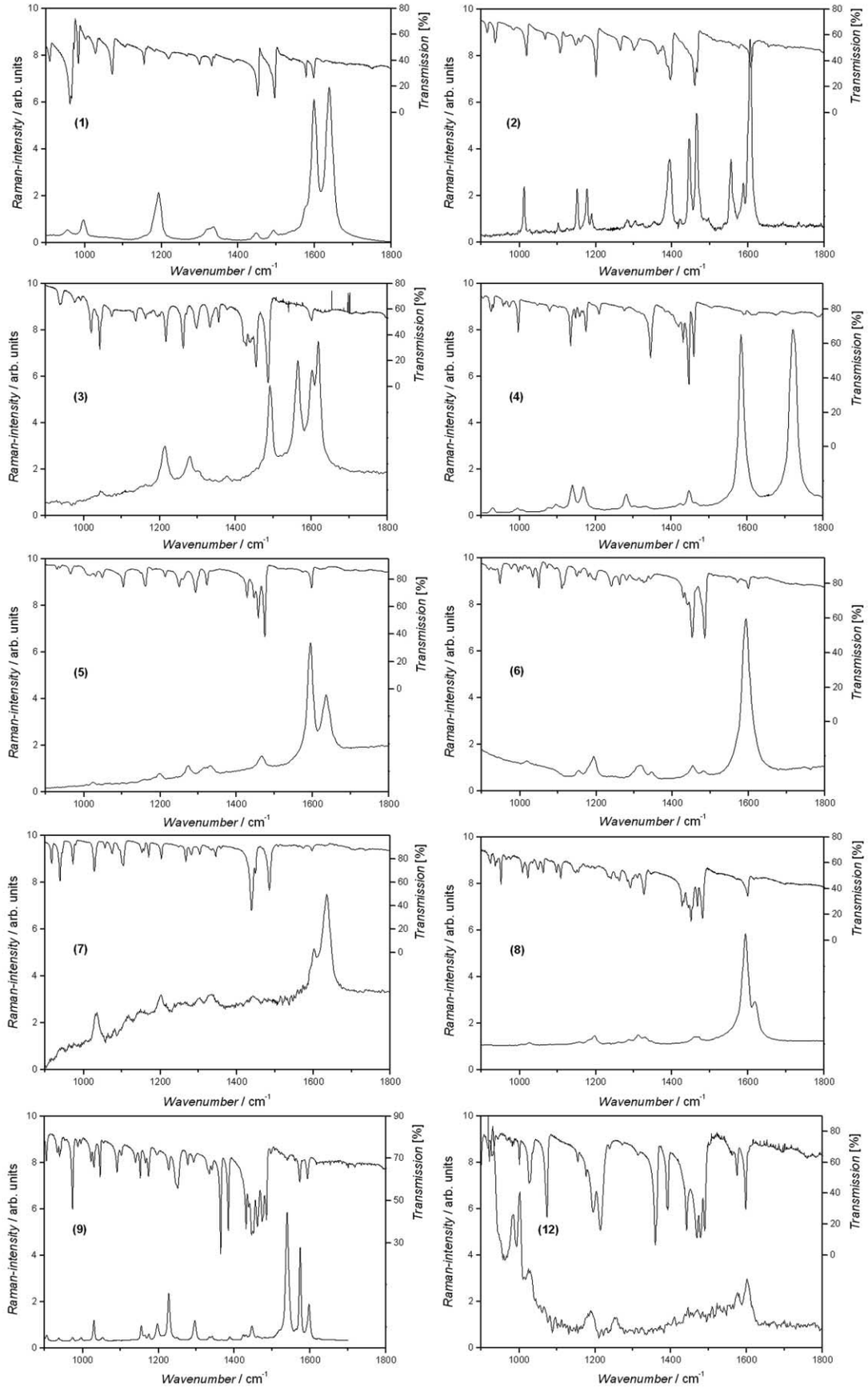

Fig. 6 IR (KBr discs) and Raman spectra (in CCl_4).

vinylic stretch. This large bathochromic shift can be related to the larger torsion angle around the double bond and the concomitantly reduced bond strength as reflected in the increased calculated bond length. The calculations predict, however, no significant bathochromic shift for **9** if compared to **6**. Noteworthy in addition is that the doublet observed in the IR spectrum of **6** is split into a series of at least 5 bands of major intensity for **9**. The strong IR bands around 1360 and 1385 cm^{-1} should be due to the methyl groups, since they appear also in the spectrum of **11**.

Table 2 Comparison of observed and calculated (in parentheses) normal mode frequencies (in cm^{-1}) in the double bond stretching region

Compound		Raman						IR			
		Vinylic		8a *sym*		8b *sym*		8a *anti*		8b *anti*	
1		1638	(1649)	1598	(1590)	1578	(1574)	1597	(1595	1578	(1575)
2		1554	(1547)	1604	(1617)	1588	(1586)	1606	(1627)	1576	(1596)
3	C_i	1617	(1647)	1600	(1595)	1563	(1575)	1600	(1599)	—	(1576)
	C_c		(1648)		(1594)		(1575)		(1597)		(1575)
4		1718	(1831)	1584	(1635)	—	(1616)	—	(1651)	—	(1635)
5		1633	(1708)	1594	(1610)	—	(1589)	1597	(1612)	—	(1590)
6	C_1	1610	(1679)	1591	(1597)	—	(1572/1577)[a]	1599	(1598)	1571	(1572/1577)[a]
	C_2		(1669)		(1593)		(1574)		(1593)		(1574)
7		1634	(1690)	1599	(1594)	1592	(1576)	1596	(1595)	—	(1576)
8		1618	(1685)	1593	(1611/1595)[a]	—	(1587/1573)[a]	1599	(1611/1595)[a]	—	(1587/1573)[a]
9		1538	(1610)	1597	(1590)	1573	(1575)	1597	(1592)	1572	(1577)
10		—	(1667)	1591	(1594)	1573	(1570)	1608	(1595)	1565	(1569)
11		1523	(1608)	1596	(1591)	1573	(1569)	1604	(1592)	1570	(1570)
12		—	(1655)	1601	(1587)	1575	(1570)	1595	(1592)	1574	(1568)

[a] The phenyl-modes are localized on only one phenyl ring; the values represent the two frequencies of the individual modes.

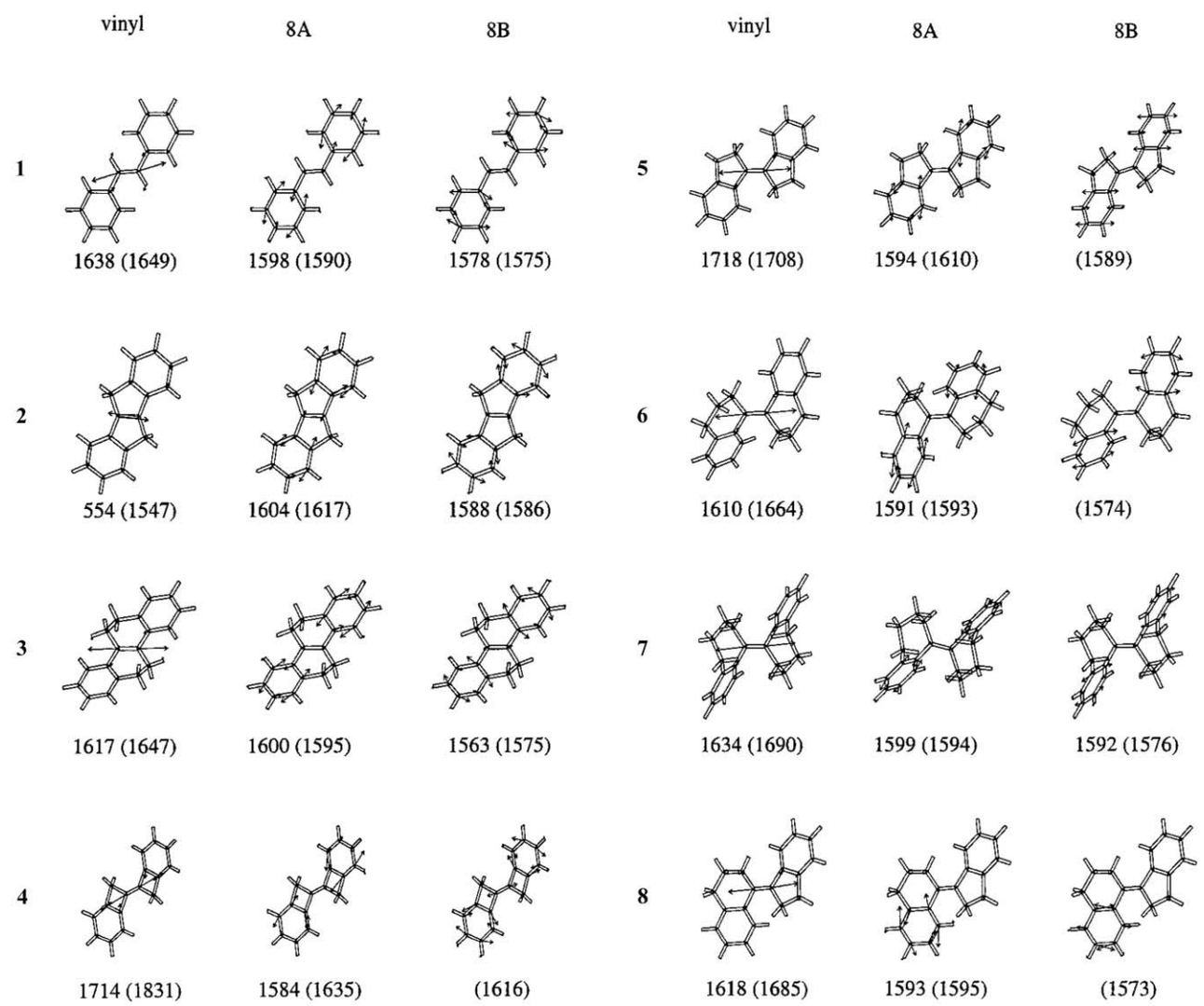

Fig. 7 A selection of calculated normal modes of **1**–**8**. Left: vinylic stretch; center: modes based on 8a benzene modes; right: modes based on 8b benzene modes. Numbers refer to the observed Raman and calculated (in parentheses) band positions (in cm^{-1}).

Both phenyl modes are strong again in the methoxy derivatives **10** and **11** (not shown), thus providing additional evidence that local symmetry (substitution pattern) is an important parameter for the determination of the IR intensities. Furthermore, the change in band pattern observed in the Raman spectra for the pair **6** and **9** is also found for the pair **10** and **11**. Whereas in **10** only one strong band is seen around 1596 cm^{-1} and a weak shoulder around 1573 cm^{-1}, a series of three bands is observed in the Raman spectrum of **11**. The one close to 1530 cm^{-1} shows also no counterpart in the IR spectrum and is therefore assigned to the vinylic stretching mode.

It is worth mentioning that in the mixed 5/6-ring derivative **8**, only one phenyl stretching band can be observed in the IR spectrum with medium intensity. In the Raman spectrum, the

phenyl vibration is found in the expected region at 1593 cm^{-1}, the weak vinyl stretching band at 1618 cm^{-1}. In both cases, the bands are at significantly lower frequencies than in **5**. When comparing the sequence **4**, **5**, **8** and **6**, it must be concluded that the vinyl vibration in **6** should be of very low intensity and at a frequency close to that of the phenyl mode. Based on this assumption, we assign the weak shoulder observed in the spectrum of **6** around 1610 cm^{-1} as a very weak vinylic stretching vibration.

In summary, the introduction of the aliphatic bridges does not significantly influence the frequency of the C=C-stretching vibration of the phenyl rings, but alters the frequency of the vinylic stretch and its intensity relative to that of the phenyl vibration. Except in the case of compound **4**, in which the vinylic stretch mode exhibits a hypsochromic shift of about 80 cm^{-1} one generally finds a bathochromic frequency shift which does not exceed 25 cm^{-1} except for compound **2** (−80 cm^{-1}). The model calculations, however, are not capable of predicting the observed shifts correctly. One could suspect from inspection of the normal mode pictures (Fig. 6) that the deviations are caused by the inadequate description of the movement of those atoms which constitute the bridging ring. Their contributions are largest in the 4-ring derivative, for which the differences between experimentally and calculated frequencies are largest (including the results for the phenyl vibrations). It has been reported earlier that the parameterization of the PM3 hamiltonian is not well suited for a proper description of molecules containing small rings with high tension.[28] This handicap could also affect the proper description of the "exocyclic" double bond. Despite the errors in the calculation of the normal mode frequencies, one can assume that the normal mode pictures give a fair representation of the discussed modes. They confirm the great similarity of the five modes observed in the double bond stretching region throughout the various derivatives and provide a rationale for the observation that the phenyl modes show only small frequency shifts.

Time-resolved fluorescence

It has been pointed out before that those substitutions which constrain the twisting of the phenyl rings change the spectral features of the fluorescence in such a way that they become more similar to those of **1** at very low temperature and in a viscous environment.[1] Nevertheless, the isomerization rate is not inhibited by this constraint, it even increases.[18,20,29] In Table 3, we have compared the fluorescence decay times of *trans*-stilbene **1** with those of **4** and **5** in various solvents at ambient temperature. Whereas the above statement is true for derivative **5** (Rothenberger and co-workers reported a lifetime of 26 ps for **5** in *n*-hexadecane[20]), the decay of **4** is slowed down by roughly a factor of 2 compared to that of stilbene **1**. It should be noted that the lifetime data of **5** could be determined only because the decay appears mono-exponential in contrast to that of **4** and *trans*-stilbene. In the latter samples, the relative amplitudes of the second and third component increase with increasing time of irradiation by the exciting ps-laser pulses (this is confirmed by repetitively reading out the decay curves), for which reason they are assigned to the *cis*-isomer (in the case of **4**) and photoproducts present in the sample. It is well known (see above) that one of the primary photoproducts of *cis* stilbene is dihydrophenanthrene, which is easily oxidized to phenanthrene. The reported lifetime of phenanthrene is about 60 ns,[19] the one of 9,10-dihydrophenanthrene was determined as 6.2 ns in *n*-hexane. Therefore, the longer-lived component found in the *trans*-stilbene sample (τ_3 = 6.1 ns) can be assigned to 9,10-dihydrophenanthrene; the origin of the shorter-lived one (τ_2 = 1.4 ns) is unclear. An inspection of the GC/MS of the irradiated sample of *trans*-stilbene revealed a larger number of photoproducts, but only two with major intensity. Of these, one could be assigned to phenanthrene due to its fragmentation pattern. It is interesting to note that the photoproduct of **4** exhibits essentially the same fluorescence decay time as the unidentified photoproduct from *trans*-stilbene. Therefore, the photochemical decay channel leading to this product should not be altered by introduction of the 4-membered ring. At ambient pressure, the fluorescence lifetime of the *cis*-isomer of **4** is also increased *vs.* that of *cis*-stilbene. In the nonpolar solvents, we find values of approximately 50 ps (*n*-hexane). Due to the decrease of this lifetime with applied pressure, its value drops below our time resolution.[32]

Table 3 Comparison of fluorescence decay times (in ps) of **1** (λ_{det} = 350 nm), **4** (λ_{det} = 350 nm) and **5** (λ_{det} = 370 nm) in various solvents. λ_{ex} = 308 nm[a]

Solvent	1	4	5
n-Hexane	83	140	22
Methylcyclohexane	79	120	29
MeOH	48	100	21
MeCN	43	100	15

[a] Lifetimes of additional photoproduct are discussed in the text.

For completeness it should be mentioned that the fluorescence of the photoproducts of **10** and **11** can be fitted bi-exponentially with a lifetime being nearly the same and equal to that of the unknown photoproducts of stilbene **1** and derivative **4** (τ_F ~ 1.4 ns). One can therefore speculate whether the newly formed chromophore has a similar structure with respect to the π-electron system. It should also be mentioned that the variable temperature studies showed that the lifetime of the shorter-lived component was essentially independent of the temperature whereas the longer one (τ_2 = 15.4 ns for **10** and 7.2 ns for **11**) increased by 50% (T ~ 150 K). This suggests that the photoproduct with the shorter fluorescence decay time has a fairly rigid structure.

Summary and conclusion

In order to investigate the influence of torsion around the single bond on the excited state kinetics of *trans*-stilbene, a number of derivatives in which this torsion is hindered by aliphatic bridges of variable size were synthesized and investigated. It was found that the normal modes based on the 8a and 8b benzene vibrations are unaffected by these bridges, whereas the vinylic stretching vibration experiences frequency shifts which cannot be explained by the results of the present quantum chemical model calculations. It turned out that all derivatives with bridges containing more than two methylene units exhibit no detectable fluorescence; methoxy substitution amplifies the importance of the photochemical decay channel similar to that observed in *cis*-stilbene (*i.e.* formation of dihydrophenanthrene and further on of phenanthrene).

It should be noted that access to these derivatives can not only help in the understanding of the photoinduced isomerization of stilbenes, but can also be advantageous with respect to the structure of the corresponding radical ions. The resonance Raman spectra of the anion and cation of *trans*-stilbene generated by photoinduced electron transfer differ to a much greater extent than one would expect on the basis of simple MO-considerations (pairing properties of HOMO and LUMO) or even by the results of *ab initio* calculations.[30] This finding can be rationalized if different geometrical relaxations are assumed for both ions. Some evidence for a geometry relaxation in the anions was provided by the differences in the transient absorption spectra of the radical ions of stilbene and its bridged derivatives.[31] Investigation of these novel cyclic stilbenes by time-resolved Raman spectroscopy can therefore shed more light on this fundamentally important question.

Experimental

General

trans-Stilbene **1** was purchased from Fluka (*scintillation grade*). Compounds **5**,[6c] **6**,[7] **9**[7] and **12**[8] were prepared as described in the literature. All other stilbene derivatives (except **2** and **3**) were prepared from the corresponding ketones by McMurry coupling.[9] Solvents were used as provided by the suppliers: *n*-hexane (Ferak or Kanto Chemical), methylcyclohexane (Aldrich), acetonitrile (Sigma-Aldrich) and methanol (Ferak), respectively.

Column chromatography was carried out using Merck Silica gel 60 (0.015–0.040 mm). Melting points were determined using a Büchi SMP-20 melting point apparatus and are uncorrected. NMR spectra were recorded on a Bruker AC 250 (250 MHz ^{1}H frequency), or with 5 mm broadband and inverse probes on a Bruker AC 400 (400 MHz ^{1}H frequency) and DMX 500 (500 MHz ^{1}H frequency) instruments, equipped with a Eurotherm BVT-2000 temperature control unit. Chemical shift values are referred to solvent resonances: DMSO-d_6 (39.50/2.49 ppm), D_3CNO_2 (62.80/4.33 ppm) and THF-d_8 (2.58 ppm); the chemical shifts δ are given in ppm; coupling constants J in Hz. Phase sensitive (TPPI) NOESY t_{mix} = 50, 450 ms and HSQC and absolute value DQF-COSY NMR spectra were recorded using Bruker standard software, using average resolution (aq (F2) = 275 ms; 256 F1 increments). Chemical shift values for assignment purposes were calculated with the ACD (Advanced Chemistry Development, Science Serve, Pegnitz, Germany) Predictor, version 5.0. Mass spectra (EI unless otherwise noted) were recorded on an HP 5989 A MS Engine. Elemental analysis was performed by Fa. Pascher, Andernach, Germany. For the irradiation experiment a super high-pressure mercury lamp HX-500 (Wacom) equipped with a bandpass filter 300FS10-50 (Andover) and a water filter (5 cm quartz cell) was used. The course of the irradiation was followed by UV/Vis spectroscopy using a Shimadzu UV-3101PC spectrophotometer. Spectra were recorded after the absorption of the dihydrophenanthrene had disappeared (*ca.* 15 min after each irradiation step). X-ray structure analyses were performed on a Nonius-Kappa-CCD diffractometer.

Raman spectra

Raman spectra were recorded on a laboratory-built apparatus as described elsewhere.[32a] The excitation source was an Ar^+ laser (Coherent, model INNOVA 90-6) for excitation wavelengths λ_{ex} = 514 and λ_{ex} = 488 nm or an eximer laser pumped dye laser (Lambda Physik EMG 102 and FL2002) for λ_{ex} = 380 nm. The Raman scattered light was observed in a back scattering arrangement, dispersed by a Jobin-Yvon model DHR 320 double spectrograph and recorded with a gated diode array (Spectroscopy Instruments, model IRY 700). For additional suppression of the exciting light, a notch filter (Kaiser Optical Systems) was placed in front of the entrance slit of the spectrograph.

Fluorescence decay curves

Fluorescence decay curves were recorded on a laboratory-built SPT-instrument using the frequency-doubled output of a cavity-dumped, synchronously pumped dye laser (t_p ~ 10 ps, *rep.* rate 800 KHz). The fluorescence was dispersed by a Zeiss monochromator and detected by a channel plate multiplier (Fa. Europhoton, Berlin, model ELDY EM1). In combination with conventional electronics (Tennelec/Ortec) an fwhm (full width at half maximum) of the instrument response function of less than 100 ps was achieved. Data analysis was performed by the usual least-squares fitting procedure assuming a multi-exponential decay law. Steady-state fluorescence spectra were recorded at the same excitation wavelength (308 nm) on a Perkin Elmer model LS50 spectrofluorimeter. Oxygen was carefully removed from the solutions *via* purging with argon for an extended period of time.

Quantum-chemical model calculations

Quantum-chemical model calculations aiming at ground state geometries were performed with the program package VAMP using PM3 Hamiltonian. The normal mode analysis uses the optimized geometry and a standard force field as implemented in the program VAMP.[33] Instead of scaling-down the calculated vibrational frequencies, we applied a scaling factor to the force constants of all internal coordinates which involve the movement of second row atoms according to eqn. (1)

$$f'_{ij} = f_{ij} * \sqrt{\phi_i} * \sqrt{\phi_j} \quad (1)$$

with ϕ_i = 1 for hydrogen and ϕ_j = 0.78 for carbon atoms and f_{ij} = standard force field (for more details see [34]). Excited state energies were calculated using all singly and doubly excited configurations generated from at least the five highest occupied and five lowest unoccupied MOs.

Syntheses

5,10-Dihydroindeno[2,1-*a*]indene 2. Compound **2** was prepared by a method described by Wawzonek,[5] and was obtained after flash chromatography (eluent: *n*-hexane–20–50% dichloromethane). Mp 208–210 °C (lit.,[5] 204–208 °C); δ_H (250 MHz; $CDCl_3$) 3.63 (4 H, s, 5-H), 7.18 (2 H, dt, *J* 7.5 and 1.2, 2-H), 7.30 (2 H, dt, *J* 7.5 and 1.1, 3-H), 7.42 (2 H, d, *J* 7.3, 4-H) and 7.50 (2 H, d, *J* 7.5, 1-H); δ_C (62 MHz; $CDCl_3$) 32.7 (t, 2 × C-5), 119.1 (d, 2 × C-4), 124.5 (d, 2 × C-2), 124.7 (d, 2 × C-1), 126.6 (d, 2 × C-3), 141.4 (s, 2 × C-4a), 147.3 (s, 2 × C-5a) and 150.8 (s, 2 × C-4b).

5,6,11,12-Tetrahydrochrysene 3. Compound **3** was synthesized according to Lyle and Daub,[6b] and was obtained after flash chromatography (eluent: *n*-hexane–0.5% ethyl acetate) and recrystallization from methanol as colorless crystals. Mp 105 °C (lit.,[6a] 105 °C); δ_H (250 MHz; $CDCl_3$) 2.70 (4 H, t, 4-H, 11-H), 2.90 (4 H, t, 6-H, 12-H) and 7.25 (8 H, m, $H_{arom.}$).

***trans*-1-(1-Benzocyclobutenylidene)benzocyclobutene 4.** The McMurry reagent was prepared in the following way:[9] $TiCl_4$ (0.77 mL, 7 mmol) and subsequently zinc powder (1.33 g, 4 mmol) were carefully added at 0 °C to anhydrous THF (75 mL) under nitrogen. A solution of benzocyclobuten-1-one[35] (0.71 g, 6 mmol) in THF (25 mL) was added and the resulting black slurry was refluxed for 21 h. After cooling to rt, the reaction mixture was treated with 10% aqueous K_2CO_3 solution (75 mL). The mixture was extracted with diethyl ether (4 × 50 mL), the organic phase washed with water, dried over $MgSO_4$, and the solvent evaporated *in vacuo*. The crude product (0.72 g of a 40 : 60 mixture of diol **13** and **4**) was purified by chromatography (50 g silica gel; eluent: *n*-hexane–10% acetone). ***trans*-4** and ***cis*-4** (0.42 g, 22%) were obtained as a 1 : 1 mixture as shown by GC/MS analysis. A small amount of the isomeric mixture was separated by semipreparative HPLC (Gilson 350; Merck LiChrospher column RP18, particle size 5 μ; eluent: acetonitrile–water 2 : 1). Pure ***trans*-4** was alternatively obtained as colorless prisms *via* recrystallization from *n*-hexane–methanol. Mp 181–183 °C; δ_H (400 MHz; $CDCl_3$) 3.80 (4 H, s, 2-H) and 7.11–7.33 (8 H, 2 × m, $H_{arom.}$); δ_C (100 MHz; $CDCl_3$) 37.6 (t, 2 × C-2), 118.8 (d, 2 × C-6), 122.7 (d, 2 × C-5), 127.5 (s, 2 × C-1), 128.1 and 127.5 (2 × d, 2 × C-3, 2 × C-4) and 145.0 and 144.9 (2 × s, 2 × C-2a, 2 × C-6a); *m*/*z* 204 (M^+, 74%), 203 (100), 202 (97), 201 (16) and 101 (1/2 $M^+ - 1$, 11). Found: C, 93.89; H, 6.30. Calc. for $C_{16}H_{12}$: C, 94.07; H, 5.92%.

7,7'-Dihydroxy-7-bicyclo[4.2.0]octa-1,3,5-trien-7-ylbicyclo-[4.2.0]octa-1,3,5-triene 13. δ_H (400 MHz; $CDCl_3$) 1.53 (2 H, br s,

OH), 3.04 (2 H, d, *J* 14.4, 2-H), 3.17 (2 H, br s, 1-H), 3.30 (2 H, d, *J* 14.4, 2-H) and 7.01–7.18 (8 H, br m, $H_{arom.}$); δ_C (100 MHz; $CDCl_3$) 42.7 (t, 2 × C-2), 82.9 (d, 2 × C-1), 121.4 (d, 2 × $C_{arom.}$), 123.2 (d, 2 × $C_{arom.}$), 127.1 (d, 2 × $C_{arom.}$), 129.5 (d, 2 × $C_{arom.}$), 142.3 (s, 2 × $C_{arom.}$) and 146.8 (s, 2 × $C_{arom.}$).

Indane-tetramer 14. From the crude reaction mixture of **4**, **14** was obtained after column chromatography (eluent: *n*-hexane–0.5% ethyl acetate) and recrystallization from methanol as colorless cubes. Mp 143–145 °C; δ_C (100 MHz; THF-d_8; 253 K) 30.3 (2 × t), 32.2 (t), 34.4 (t), 36.2 (t), 37.4 (t), 50.0 (d), 58.9 (d), 123.2, 123.4, 123.8, 124.0, 124.2, 124.4, 124.6, 124.8, 125.0, 125.5, 125.7, 125.8, 125.9, 126.7, 126.8, 127.1, 130.9, 137.8, 138.9, 141.9, 144.6, 144.7, 145.0, 145.4, 145.8, 147.1, 147.6 and 150.2; *m*/*z* (EI)‡‡ 230 (1/2 M^+ − 1, 86%), 229 (49), 228 (26) and 115 (100); *m*/*z* (CI) 463 (M^+, 1%), 234 (20), 233 (100), 232 (50), 230 (95) and 117 (15). Found: C, 93.46; H, 6.53. Calc. for $C_{36}H_{30}$: C, 93.21; H, 6.76%.

***trans*-1-(1-Benzocycloheptenylidene)benzocycloheptene 7.** The McMurry reagent (*vide supra*) was prepared from 8.0 mL $TiCl_4$ (26 mmol) and 3.4 g zinc powder (50 mmol) in 200 mL anhydrous THF. 3.84 g 1-benzosuberone (24.0 mmol), dissolved in 50 mL THF, were added and the mixture was refluxed for 22 h. After the usual work-up 3.2 g of crude product were obtained, which was purified by chromatography (eluent: *n*-hexane–5% acetone). As the less polar fraction, 0.92 g (27%) of ***trans*-7** were obtained as colorless prisms after recrystallization from *n*-hexane. Mp 179–180 °C; δ_H (400 MHz; THF-d_8; 253 K) 1.35 (4 H, br quintet, CH_2), 1.60–1.78 (2 H, br m, CH_2), 1.85–1.95 (4 H, br m, CH_2), 2.65–2.69 (4 H, m, CH_2), 3.0 (2 H, br dt, CH_2), 7.10–7.25 (6 H, m, $H_{arom.}$) and 7.38 ppm (2 H, d, $H_{arom.}$); δ_C (100 MHz; D_3CNO_2; 363 K) 27.9 (t, 2 × C-4), 30.4 (br t, 2 × C-3), 32.8 (t, 2 × C-2), 36.0 (t, 2 × C-5), 126.5 and 125.8 (2 × d, 2 × C-8, 2 × C-9), 128.9 and 128.6 (2 × d, 2 × C-6, 2 × C-7), 138.6 (s, 2 × C-9a), 141.1 (s, 2 × C-5a) and 143.7 (s, 2 × C-1); *m*/*z* 288 (M^+, 100%), 245 (7), 231 (10), 217 (10), 216 (7), 215 (10), 202 (7), 145 (1/2 M^+ + 1, 54), 144 (1/2 M^+, 14), 143 (19), 142 (7), 141 (7), 129 (17), 128 (14), 117 (10), 115 (14) and 91 (10). Found: C, 91.83; H, 8.17. Calc. for $C_{22}H_{24}$: C, 91.61; H, 8.39%.

***trans*-1-(1-Indanylidene)tetralin 8.** The McMurry reagent was prepared from 2.05 mL $TiCl_4$ (18.6 mmol) and 2.44 g zinc powder (37.3 mmol) in 100 mL dry THF as solvent. To the slurry, 1.54 g of 1-indanone (11.6 mmol) and 0.85 g of 1-tetralone (5.8 mmol) dissolved in 100 mL THF were added. The mixture was refluxed for 18 h. Work-up gave 1.5 g of crude product, which was purified by chromatography (eluent: *n*-hexane–1% acetone). 80 mg (8%) **8** were obtained from the least polar fraction as colorless prismatic crystals. Mp 108–109 °C; δ_H (400 MHz; $CDCl_3$) 1.84 (2 H, q, 3-H), 2.61 (2 H, t, 4-H), 2.88 (2 H, t, 3′-H), 2.95 (2 H, dt, 2-H), 3.04 (2 H, dt, 2′-H), 7.12–7.30 (6 H, m, $H_{arom.}$), 7.45 (1 H, d, 8-H, $H_{arom.}$) and 7.65 (1 H, d, 8′-H, $H_{arom.}$); δ_C (100 MHz; $CDCl_3$) 23.8 (t, C-3), 29.1 (t, C-2), 30.2 (t, C-4), 31.1 (t, C-3′), 35.3 (t, C-2′), 124.9 (d), 125.2 (d), 125.9 (d), 126.1 (d), 126.3 (d), 127.1 (d), 127.2 (d), 128.7 (d), 129.9 (s), 138.1 (s), 138.4 (s), 140.6 (s), 142.6 (s) and 147.3 (s); *m*/*z* 246 (M^+, 100%), 215 (19), 131 (1/2 M^+ + 1 of tetralinylidene, 21) and 117 (1/2 M^+ + 1 of indanylidene, 21). Found: C, 92.41; H, 7.58. Calc. for $C_{19}H_{18}$: C, 92.63; H, 7.36%.

***trans*-1-(6-Methoxy-1-tetralinylidene)-6-methoxytetralin 10.** The McMurry reagent was prepared from 2.05 mL $TiCl_4$ (18.7 mmol) and 2.5 g zinc powder (38.2 mmol) in 150 mL anhydrous THF. 3.08 g of 6-methoxy-1-tetralone dissolved in 50 mL THF were added and the mixture was refluxed for 20 h. After the usual work-up 2.1 g of crude product were obtained. Recrystallization from ethyl acetate gave 1.23 g (41%) of **10** as small prisms. Mp 210–211 °C; δ_H (400 MHz; C_6D_6) 1.71 (4 H, quintet, *J* 6.6, 3-H), 2.63 (4 H, t, *J* 6.6, 4-H), 2.67 (4 H, t, *J* 6.6, 2-H), 3.78 (6 H, s, 2 × OCH_3), 6.65 (2 H, d, *J* 2.7, 5-H), 6.70 (2 H, dd, *J* 8.5 and 2.7, 7-H) and 7.23 (2 H, t, *J* 8.5 and 2.7, 8-H); δ_C (100 MHz; C_6D_6) 24.4 (t, 2 × C-3), 29.7 (t, 2 × C-2), 30.0 (t, 2 × C-4), 55.2 (q, 2 × OCH_3), 110.7 (d, 2 × C-7), 112.8 (d, 2 × C-8), 130.9 (s, 2 × C-8a), 131.1 (d, 2 × C-5), 131.3 (s, 2 × C-4a), 141.0 (s, 2 × C-1) and 158.3 (s, 2 × C-6); *m*/*z* 320 (M^+, 100%), 305 (M^+ − CH_3, 14), 277 (7), 199 (5), 161 (1/2 M^+ + 1, 35), 160 (1/2 M^+, 16), 147 (7), 146 (8), 145 (8), 144 (7) and 115 (9). Found: C, 82.48; H, 7.53. Calc. for $C_{22}H_{24}O_2$: C, 94.07; H, 7.54%.

***trans*-1-(2,2-Dimethyl-6-methoxy-1-tetralinylidene)-2,2-dimethyl-6-methoxytetralin 11.** *Synthesis of 2,2-dimethyl-6-methoxy-1-tetralone*[36]. To 28.0 g of powdered KOH (0.5 mol) were added 100 mL of toluene and 0.13 g [18]-crown-6 (0.05 mmol). To this mixture 8.8 g of 6-methoxy-1-tetralone (0.043 mol) were added. The mixture was heated to 70 °C and 16.0 mL of methyl iodide (0.188 mol) were added dropwise. After stirring for 2 h, the mixture was diluted with 200 mL H_2O. The organic phase was separated and the aqueous phase was extracted twice with diethyl ether. The combined organic phases were washed with H_2O, dried over $MgSO_4$ and evaporated *in vacuo*. The crude liquid product was purified by vacuum distillation, yielding 8.69 g of an orange colored oil (85%); bp 110 °C (0.05 Torr); δ_H (400 MHz; C_6D_6) 1.12 (6 H, s, 2 × CH_3), 1.57 (2 H, t, *J* 6.4, 3-H), 2.50 (2 H, t, *J* 6.4, 4-H), 3.21 (3 H, s, OCH_3), 6.45 (1 H, dd, *J* 2.7 and 1.0, 5-H), 6.59 (1 H, dd, *J* 0.5 and 2.5, 7-H) and 8.34 (1 H, d, *J* 8.5 Hz, 8-H); δ_C (100 MHz; C_6D_6) 24.6 (q, 2 × CH_3), 26.1 (t, C-3), 36.8 (t, C-4), 41.2 (s, C-2), 54.8 (q, OCH_3), 113.0 (d, C-7), 113.1 (d, C-8), 125.8 (s, C-4a), 130.8 (d, C-5), 145.5 (s, C-8a), 163.5 (s, C-6) and 200.1 (s, C=O); *m*/*z* 204 (M^+, 33%), 189 (10, M^+ − CH_3), 161 (9, 189 − CO), 148 (100), 120 (17) and 91 (10). Found: C, 76.64; H, 7.68. Calc. for $C_{26}H_{32}O_2$: C, 76.44; H, 7.89%.

McMurry coupling[37]. The McMurry reagent was prepared from 2.4 mL $TiCl_3$ (15.6 mmol) in 100 mL THF and 0.3 g $LiAlH_4$ (7.8 mmol), which was slowly added. After the mixture was refluxed for 15 min, 1.6 g of 2,2-dimethyl-6-methoxy-1-tetralone (7.8 mmol) dissolved in 50 mL THF was added and the mixture was refluxed again for 52 h. After the usual work-up procedure the crude product was purified by chromatography (100 g silica gel; eluent: *n*-hexane–10% ethyl acetate). After crystallization from *n*-hexane 0.24 g of pure **11** (18%) were obtained as white needles; mp 140–141 °C; δ_H (400 MHz; $CDCl_3$) 0.79 (6 H, s, 2 × CH_3), 1.10 (6 H, s, 2 × CH_3), 1.47 (4 H, br dt, 3-H), 2.70 (4 H, t, *J* 4.5, 4-H), 3.76 (6 H, s, 2 × OCH_3), 6.59 (2 H, dd, *J* 2.8, 5-H), 6.76 (2 H, d, *J* 8.1, 7-H) and 7.09 (2 H, d, *J* 8.3, 8-H); δ_C (100 MHz; $CDCl_3$) 26.4 (t,. 2 × C-3), 30.8 (2 × q, 4 × CH_3), 31.2 (t, 2 × C-4), 33.0 (s, 2 × C-2), 55.1 (q, 2 × OCH_3), 112.7 (d, 2 × C-7), 123.7 (s, 2 × C-8a), 131.6 (d, 2 × C-5), 133.8 (s, 2 × C-4a), 136.9 (s, 2 × C-1) and 157.3 (s, 2 × C-6); *m*/*z* 376 (M^+, 100%), 361 (M^+ − CH_3, 30), 320 (19), 305 (60), 291 (10), 290 (14), 289 (17), 255 (16), 173 (17, 1/2 M^+), 147 (13) and 115 (9). Found: C, 82.60; H, 8.90. Calc. for $C_{26}H_{32}O_2$: C, 82.93; H, 8.57%.

Acknowledgements

The authors wish to thank Dr J. Schröder and Dr D. Schwarzer (Göttingen) for many stimulating discussions. Financial support by the Deutsche Forschungsgemeinschaft and the Fonds der Chemischen Industrie is also gratefully acknowledged, and so is the donation of a sample of benzocyclobutenone by Professor P. Schiess from the University of Basel. We also appreciate Dr B. Sägmüller′s, Dipl.-Chem. G. Trachta′s

‡‡ In an earlier report, the structure was incorrectly assigned to a biindenyl derivative based on its EI MS spectra.[6c]

and Professor J. E. Gano′s help in the preparation of this manuscript.

References

1 For some recent reviews see: (*a*) H. Görner and H. J. Kuhn, *Adv. Photochem.*, 1995, **19**, 1; (*b*) D. H. Waldeck, *Chem. Rev.*, 1991, **91**, 415; (*c*) T. Majima, S. Tojo, A. Ishida and S. Takamuku, *J. Phys. Chem.*, 1996, **100**, 13615; (*d*) H. Meier, *Angew. Chem.*, 1992, **104**, 1425; H. Meier, *Angew. Chem., Int. Ed. Engl.*, 1992, **31**, 1399; (*e*) J. Saltiel and Y.-P. Sun, in *Photochromism: Molecules and Systems*, ed. H. Dürr and H. Bouas-Laurent, Elsevier, Amsterdam, 1990, p. 64; (*f*) J. Saltiel, J. D'Agostino, E. D. Megarity, L. Metts, K. R. Neuberger, M. Wrighton and O. C. Zafiriou, *Org. Photochem.*, 1973, **3**, 1.

2 *E.g.* (*a*) S. Schneider, B. Brem, W. Jäger, H. Rehaber, B. Mantel, D. Lenoir and R. Frank, *Chem. Phys. Lett.*, 1999, **308**, 211; (*b*) K. Ogawa, M. Futakami, H. Suzuki and A. Kira, *J. Chem. Soc., Perkin Trans. 2*, 1988, 2115; (*c*) J. Vogel, S. Schneider, F. Dörr, P. Lemmen and D. Lenoir, *Chem. Phys.*, 1984, **90**, 387; (*d*) J. Saltiel, A. D. Rousseau and B. Thomas, *J. Am. Chem. Soc.*, 1983, **105**, 7631.

3 (*a*) N. Koumura, R. W. J. Zijlstra, R. A. van Delden, N. Harada and B. L. Feringa, *Nature*, 1999, **401**, 152; (*b*) N. Harada, N. Koumura and B. L. Feringa, *J. Am. Chem. Soc.*, 1999, **119**, 7256.

4 Y. Yoshimura and K. Tsujimoto, *presented at the 79th National Meeting of the Chemical Society of Japan*, Kobe, 2001; *Book of Abstracts*, p. 727.

5 S. Wawzonek, *J. Am. Chem. Soc.*, 1940, **62**, 745.

6 (*a*) W. Salzer, *Hoppe-Seyler's Z. Physiol. Chem.*, 1942, **274**, 39; (*b*) T. A. Lyle and G. H. Daub, *J. Org. Chem.*, 1979, **44**, 4933; (*c*) D. Lenoir and P. Lemmen, *Chem. Ber.*, 1980, **113**, 3112.

7 P. Lemmen and D. Lenoir, *Chem. Ber.*, 1984, **117**, 2300.

8 D. Lenoir and H. Burghard, *J. Chem. Res. (S)*, 1980, 386; D. Lenoir and H. Burghard, *J. Chem. Res. (M)*, 1980, 4715.

9 (*a*) D. Lenoir, *Synthesis*, 1989, 883; (*b*) J. McMurry, *Chem. Rev.*, 1989, **89**, 1513.

10 (*a*) R. Frank, PhD Thesis, Technische Universität München, 1994; (*b*) J. Lex, J. Neudörfl, P. Lemmen and M. Oelgemöller, *unpublished results.*

11 O. Ermer, *Aspekte von Kraftfeldrechnungen*, Baur Verlag, München, 1981.

12 (*a*) N. L. Allinger and J. T. Sprague, *J. Am. Chem. Soc.*, 1972, **94**, 5734; (*b*) U. Burkert and N. L. Allinger, *Molecular Mechanics ACS Monograph 177*, ACS, Washington D.C., 1982; (*c*) G. Favini, G. Buemi and M. Raimondi, *J. Mol. Struct.*, 1968, **2**, 137; (*d*) R. Pauncz and D. Ginsberg, *Tetrahedron*, 1960, **9**, 40.

13 K. Ogawa, H. Suzuki, M. Futakami, S. Yoshimura, T. Sakurai, K. Kobayashi and A. Kira, *Bull. Chem. Soc. Jpn.*, 1988, **61**, 939 . We thank the crystallographic reviewer for bringing this publication to our attention.

14 A. Lachapelle and M. St. Jacques, *Tetrahedron*, 1987, 5033.

15 A. Entrena, J. Campos, J. A. Gòmez, M. A. Gallo and A. Espinosa, *J. Org. Chem.*, 1997, **62**, 337.

16 (*a*) J. E. Gano, C. Kluwe, K. Kirschbaum, A. A. Pinkerton, P. Sekher, E. Skrzypczak-Jankun, G. Subramaniam and D. Lenoir, *Acta Crystallogr., Sect. C*, 1997, **53**, 1723; (*b*) J. E. Gano, B. S. Park, G. Subraniam, D. Lenoir and R. Gleiter, *J. Org. Chem.*, 1991, **56**, 4806; (*c*) D. Lenoir, J. E. Gano and J. McTague, *Tetrahedron Lett.*, 1986, 5339; (*d*) J. E. Gano, B. S. Park, A. A. Pinkerton and D. Lenoir, *J. Org. Chem.*, 1990, **55**, 2688; (*e*) J. E. Gano, B.-S. Park, A. A. Pinkerton and D. Lenoir, *Acta Crystallogr., Sect. C*, 1991, **47**, 162.

17 (*a*) J. Bernstein, *Acta Crystallogr., Sect. B*, 1975, **31**, 1268; (*b*) J. Jovanovic, M. Schürmann, H. Preut and M. Spiteller, *Acta Crystallogr., Sect. E*, 2001, **57**, o1100.

18 J. Saltiel and J. T. D'Agostino, *J. Am. Chem. Soc.*, 1972, **94**, 6445.

19 S. L. Murov, J. Carmichael and G. L. Hug, *Handbook of Photochemistry*, 2nd edn., Marcel Dekker, New York, 1993.

20 (*a*) J. Schröder, *Habilitation*, Universität Göttingen, 1991; (*b*) G. Rothenberger, D. K. Negus and R. M. Hochstrasser, *J. Chem. Phys.*, 1983, **79**, 5360.

21 (*a*) G. Hohlneicher, I. Kautz, B. Tillmanns, D. Lenoir and R. Frank, *J. Mol. Struct.*, 1995, **348**, 191; (*b*) G. Hohlneicher, R. Wrzal, D. Lenoir and R. Frank, *J. Phys. Chem. A*, 1999, **103**, 8969.

22 (*a*) F. B. Mallory and C. W. Mallory, *Org. React. (N. Y.)*, 1984, **30**, 1; (*b*) W. H. Laarhoven, *Org. Photochem.*, 1989, **10**, 163.

23 Detailed studies on the *trans–cis* photoisomerization of cyclic stilbenes will be published independently.

24 G. Varsanyi, *Vibrational Spectra of Benzene Derivatives*, Academic Press, New York, 1969.

25 G. Baranovic, Z. Meic, H. Güsten, J. Mink and G. Keresztury, *J. Phys. Chem.*, 1990, **94**, 2833.

26 A. C. Albrecht, *J. Chem. Phys.*, 1961, **34**, 1476.

27 G. Hohlneicher, personal communication.

28 J. Stewart, *J. Comput. Chem.*, 1989, **10**, 221.

29 (*a*) M. Lee, A. J. Bain, P. J. McCarthy, C. H. Ilan, J. N. Haseltine, A. B. Smith III and R. M. Hochstrasser, *J. Chem. Phys.*, 1986, **85**, 4341; (*b*) J. Schröder, *Habilitation*, Universität Göttingen, 1991.

30 (*a*) S. Schneider, Ch. Scharnagl, R. Bug, G. Baranovic and Z. Meic, *J. Phys. Chem.*, 1992, **96**, 9748; (*b*) S. Schneider, in *Time-resolved Vibrational Spectroscopy V*, ed. H. Takahashi, Springer Verlag, Berlin, 1992, p. 163.

31 H. Suzuki, K. Koyano, T. Shida and A. Kira, *Bull. Chem. Soc. Jpn.*, 1982, **55**, 3690.

32 (*a*) B. Brem, PhD Thesis, Universität Erlangen, 1998; (*b*) W. Jäger, PhD Thesis, Universität Erlangen, 1997.

33 T. Clark, G. Rauhut, A. Alex and J. Chandresekhar, *Vamp 5.5, Technical Manual*, Oxford Molecular Ltd., Oxford, 1994.

34 S. Schneider, P. Freunscht and G. Brehm, *J. Raman Spectrosc.*, 1997, **28**, 305.

35 (*a*) P. Schiess and M. Heitzmann, *Angew. Chem.*, 1977, **89**, 485; P. Schiess and M. Heitzmann, *Angew. Chem., Int. Ed. Engl.*, 1977, **16**, 469; (*b*) P. Schiess, P. V. Barve, F. E. Dussy and A. Pfiffner, *Org. Synth.*, 1995, **72**, 116.

36 M. Lissel, B. Neumann and S. Schmidt, *Liebigs Ann. Chem.*, 1987, 263.

37 S. Pogodin and I. Agranat, *Org. Lett.*, 1999, **1**, 1387.